Modelling temperature-dependent current–voltage characteristics of an MEH-PPV organic light emitting device

2002 J. Phys.: Condens. Matter 14 9925

(http://iopscience.iop.org/0953-8984/14/42/307)

INSTITUTE OF PHYSICS PUBLISHING JOURNAL OF PHYSICS: CONDENSED MATTER

J. Phys.: Condens. Matter **14** (2002) 9925–9933 PII: S0953-8984(02)36751-1

Modelling temperature-dependent current–voltage characteristics of an MEH-PPV organic light emitting device

Simon J Martin[1], J M Lupton[2], I D W Samuel[3] and Alison B Walker[1]

[1] Department of Physics, University of Bath, Bath BA2 7AY, UK
[2] Max-Planck-Institut für Polymerforschung, Ackermannweg 10, D-55128 Mainz, Germany
[3] Organic Semiconductor Centre, School of Physics and Astronomy, University of St Andrews, North Haugh, St Andrews, Fife KY16 9SS, UK

Received 9 May 2002, in final form 14 July 2002
Published 11 October 2002
Online at stacks.iop.org/JPhysCM/14/9925

Abstract

We present results from a device model in which the current–voltage (I–V) characteristics of an ITO/MEH-PPV/Al organic light emitting device have been simulated over a range of temperatures by fitting the mobilities and barrier heights. Good agreement with experimental data has been achieved at temperatures of 200–300 K at bias voltages exceeding 2 V, but there are some shortcomings of the model at lower temperatures. We have found that a discrete trap level in the simulated device improved the fit of the simulated I–V data in the low field regime at high temperatures. It has also been noted in the experimental data that cooling the device led to improved efficiency, with the ratio of light output to device current increasing by a factor of approximately 50 times when the device was cooled from 300 to 10 K. The model exhibited increased efficiency upon cooling, provided the electron barrier height, ϕ_{bn}, was decreased at a greater rate than the hole barrier height, ϕ_{bp}.

1. Introduction

During the period following the discovery of electroluminescence in organic materials, both in conjugated polymers [1] and small molecules [2], a great deal of work had been carried out on organic light-emitting devices (OLED), both in terms of trying to understand the underlying physics and to improve their performance. Considerable progress has been made in developing displays, with the application of novel techniques and materials allowing devices to be made with increased efficiencies and a range of colours. Much effort has also been made in an attempt to clarify the mechanisms of charge injection and transport in these devices. Both macroscopic device models and microscopic models have been employed to elucidate this situation. Macroscopic device models treat the organic semiconductor as a continuum band semiconductor (i.e. as a conventional inorganic semiconductor), with drift-diffusion

carrier transport in the bulk and injection at the contacts [3–6]. Such models can be used to obtain information such as current–voltage (I–V) characteristics, carrier density profiles and recombination zone profiles; these models often yield useful information but require several material parameters which are often not well known or are heavily sample-dependent.

Despite the extensive literature on macroscopic device modelling of OLEDs, very little work apart from [7–9] has been carried out to investigate the temperature-dependent behaviour of OLEDs or to validate the models over a wide temperature range. In [8, 9] the temperature-dependent I–V characteristics of a 160 nm ITO/MEH-PPV/Al device were simulated with a unipolar device model which, although similar to the models mentioned above, neglected diffusion currents. The main point made in [8, 9] was that it is essential to consider bulk transport and injection on an equal footing, otherwise spurious conclusions may be reached. This is because an apparent increase in the barrier height with temperature may be due to a reduction in the mobility, as both have the effect of reducing the current. Furthermore, Fowler–Nordheim (FN) tunnelling injection on its own was shown to be a poor explanation of the measured I–V characteristics because the barrier height decreases with increasing temperature, which is inconsistent with the fact that the bandgap is expected to increase with temperature. Furthermore, it was shown that the change in I–V curves upon intentional photo-oxidation of the polymer by exposure to intense UV irradiation cannot be explained purely on the basis of FN [8]. The inability of FN as opposed to thermionic injection to provide a realistic model of I–V curves has also been noted in [10] and [11]. However, bulk transport alone is insufficient; Malliaras *et al* [11] have noted that, even in the so-called saturation regime where the current becomes bulk limited, the slope depends on the cathode material.

The conclusions that could be drawn in [8, 9] were restricted by their model being unipolar and neglecting the diffusion current. The latter has been shown in [11] to be important when fitting I–V characteristics. In this paper, we have used a bipolar device model, including diffusion currents, to model the I–V characteristics of a 95 nm ITO/MEH-PPV/Al device over a range of temperatures from 150–300 K and to compare with experimental data to see what influence the model has on the conclusions reached.

2. Method

The device model used in this work has been described elsewhere [3, 4] and is similar to those proposed by other groups (e.g. [5, 6]). The model, which is one dimensional, bipolar and time-independent, comprises Poisson's equation, the drift-diffusion equations for carrier transport and the continuity equations. These equations are solved self-consistently, along with the appropriate boundary conditions which represent charge injection into the bulk organic material from metal contacts, by both thermionic emission over the barrier and tunnelling through the barrier. The tunnelling current density is determined from

$$I_{tun} = ACE^2 \exp\left(-\frac{8\pi\sqrt{2em\phi_{bp}^3}}{3hE}\right), \qquad C = \frac{3e^2}{8\pi h\phi_{bp}} \tag{1}$$

where E is the electric field, e is the electron charge magnitude, m is the hole effective mass (set equal to the bare electron mass), h is Planck's constant, ϕ_{bp} is the hole barrier height and A is a dimensionless fitting parameter. The model also incorporates image force lowering of the Schottky barrier and uses a field-dependent form for the carrier mobility, which accounts for the disorder inherent in the material and the hopping transport.

In organic semiconductors, it has been shown experimentally and theoretically [12] that the carrier mobility can be fitted to

$$\mu_p = \mu_{E=0} \exp\left(\sqrt{\frac{E}{E_0}}\right), \tag{2}$$

where $\mu_{E=0}$ is the zero field hole mobility and

$$\mu_{E=0} = \mu_0 \exp\left(-\frac{\Delta}{k_B T}\right), \qquad \frac{1}{\sqrt{E_0}} = B\left(\frac{1}{k_B T} - \frac{1}{k_B T_0}\right) \tag{3}$$

where μ_0 is a constant, the parameter E_0 dictates how strongly the mobility is modified by the field, Δ is the activation energy and T_0 and B are material constants related to the degree of disorder in the material. Equation (2) is often misleadingly termed the Poole–Frenkel mobility because of the square root variation with the field, although its origin and temperature variation is quite different from the form derived by Poole and Frenkel [11, 13]. Details of the experimental method are given in [8].

3. Results

The simulated I–V characteristics were fitted to the experimental data by varying μ_p, E_0, and ϕ_{bp}. This procedure yields values for the zero field hole mobility parameters which are given in table 1 and compared with published values. The conduction band density of states, N_C, was set equal to the valence band density of states, N_V, and to the density of conjugated chain segments which here is assumed to be 1×10^{21} cm^{-3} following [5, 8, 9]). The HOMO and LUMO levels of MEH-PPV are taken as being 5.4 eV [14] and 3 eV [15], respectively, giving a bandgap E_g of 2.4 eV, which agrees with [5]. The workfunction of Al is set to 4.3 eV, resulting in a barrier to electron injection ϕ_{bn} at the cathode of 1.3 eV. This parameter was allowed to vary with temperature when comparing predicted and measured efficiencies.

The workfunction of ITO varies from about 4.7 to 5.2 eV, depending upon the method of preparation, resulting in a barrier to hole injection, ϕ_{bp}, at the anode of between 0.2 and 0.7 eV. The large barrier to electron injection and the fact that MEH-PPV is known to be a preferential hole transporting material means that the electron current makes a small contribution to the total device current. The electron mobility μ_n parameters are hard to determine because electron transport is dispersive in MEH-PPV, so, strictly speaking, the mobility is an ill defined quantity and it is difficult to fit because of the electron current being so small. We have made the assumption $\mu_n = 0.01\mu_p$ as its value makes little difference to our results given the large barrier to electron injection. An exception is when we fit the electron barrier height to try to reproduce the temperature dependence of the measured efficiency, where we have also considered the case $\mu_n = 0.1\mu_p$.

The parameters derived from the fit of the tunnelling expression to the experimental data are: 300 K, $A = 5.3 \times 10^{-8}$, 290 K $A = 5.6 \times 10^{-8}$, 280 K $A = 1.5 \times 10^{-7}$, 270 K $A = 1.5 \times 10^{-7}$, 260 K $A = 5 \times 10^{-7}$, 250 K $A = 2.5 \times 10^{-7}$, 240 K $A = 5 \times 10^{-7}$, 230 K $A = 5 \times 10^{-6}$, 220 K $A = 1 \times 10^{-5}$, 210 K $A = 1 \times 10^{-4}$, 200 K $A = 1 \times 10^{-2}$. In FN theory, equation (1), A is independent of temperature. However, [16] has argued that A does depend on temperature through the changes with temperature of the Fermi distribution of the electrons in the metal contact. Even so, there is a much weaker temperature dependence than we find here. Therefore we conclude that the variation of A with temperature comes about because FN tunnelling is of dubious validity for organic devices.

Figure 1 shows the modelled and experimental I–V characteristics for temperatures of 150, 200, 250 and 300 K. At temperatures of 200–300 K in figure 1, the model provides

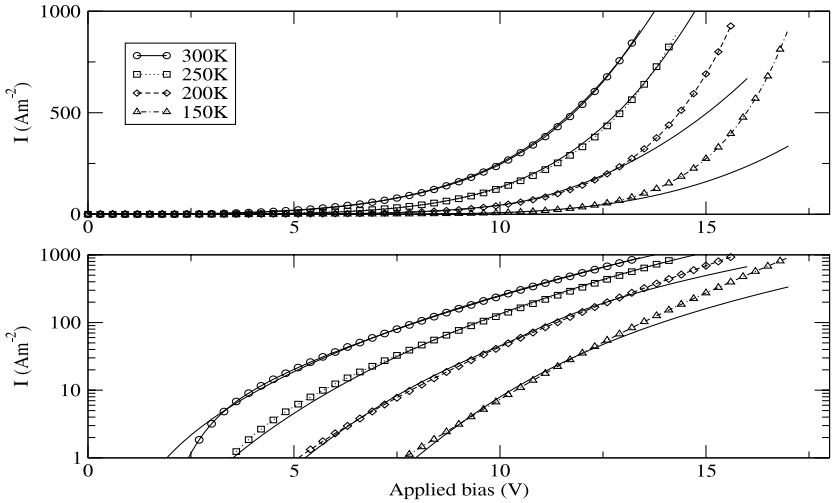

Figure 1. Experimental current densities I as a function of applied bias at temperatures of 150 K (triangles), 200 K (diamonds), 250 K (squares) and 300 K (circles) and simulated data (full curves). The top panel is a linear–linear plot and the bottom panel is a log–linear plot of the same data.

excellent agreement with the experimental data for most applied biases, but the agreement is less good as the temperature decreases and it overestimates the injected current magnitude at low biases (below about +2 V). At 150 K the fit becomes much worse below 5 V. At low biases, the model underestimates the injected current and higher biases and the current is close to that predicted by a space charge limited current (SCLC) [19]:

$$I_{SCLC} \approx \frac{9}{8}\epsilon\epsilon_0\mu_0\frac{V^2}{d^3}\exp(0.89\beta\sqrt{V/d}). \tag{4}$$

One explanation for the difficulty in obtaining a good fit at low temperatures is that the film heats up due to the current flowing through it [20], so that the I–V characteristics become steeper as the temperature is reduced.

Figure 2 shows the fitted hole barrier height (ϕ_{bp}) from the model as a function of temperature. As the temperature was decreased, the hole current injected into the MEH-PPV from the ITO was too low for all biases, so the barrier height had to be reduced slightly to increase the injected current. However, reducing the barrier height caused the injected current to be too large and so μ_p had to be reduced to compensate. The field dependence was also found to increase with decreasing temperature, as has been found experimentally, e.g. [12].

Lupton and Samuel [8, 9] found that the barrier height varied linearly with temperature with a slope of 1.2 meV K^{-1} down to about 200 K, before tailing off, and noted that this slope is a factor of nearly 2 greater than is expected from bandgap shrinkage. In figure 2, we obtain a slope of 1 meV K^{-1} and the fitted barrier height at room temperature is about 0.1 eV lower and 0.2 eV less than in [5]. An explanation for this discrepancy could come from the increased importance of an interfacial layer occurring in the spin-coating process [8] for a thinner device. Figure 3 shows the temperature dependence of the hole mobility, μ_p, and E_0.

Our values of B and T_0 result in a set of temperature-dependent I–V characteristics, which match the experimental data well, despite being lower than other values quoted in table 1. $E_0(T)$ determines the field dependence of the mobility, and hence the slope of the I–V curve at high biases before tunnelling currents become significant. Our values of Δ and μ_0 are only slightly lower than the values quoted in table 1. This may be a result of some of

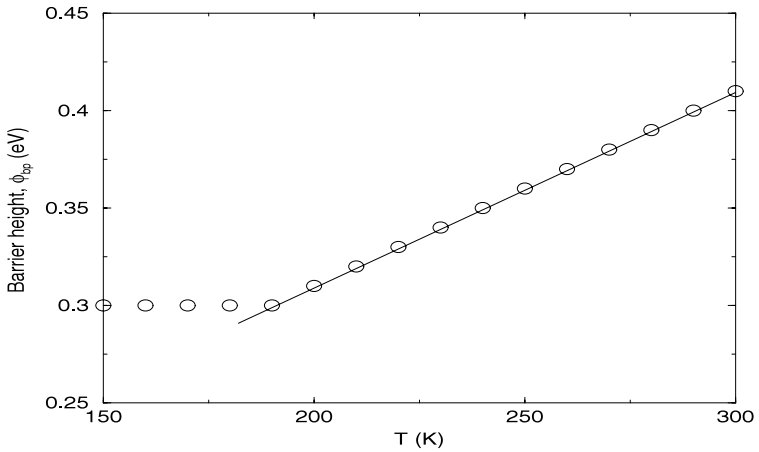

Figure 2. Fitted hole barrier height (circles) (ϕ_{bp}) as a function of temperature. The full line is a linear fit to the data.

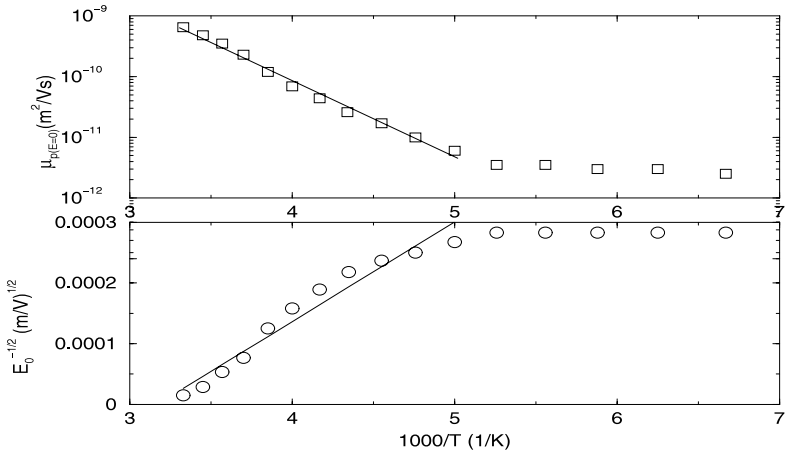

Figure 3. Arrhenius plot of $\mu_{p(E=0)}$ parameter (top panel) and $E_0^{-1/2}$ (bottom panel).

Table 1. Parameter values used for zero-field mobility $\mu_{E=0}$.

Parameter	This work	[8, 9]	[17]	[14]	[18]
Δ (eV)	0.27	0.75	0.48	0.38 ± 0.02	0.22
μ_0 (m^2 V^{-1} s^{-1})	1×10^{-5}	1.5×10^{-4}	3.5×10^{-3}	1×10^{-5}	7×10^{-7}
T_0 (K)	325	300	600	600 ± 90	430
B (eV mV$^{-1/2}$)	1.3×10^{-5}	5.5×10^{-5}	2.9×10^{-5}	$2.3 \pm 0.2 \times 10^{-5}$	2.9×10^{-5}

the temperature dependence of the mobility being lost due to the strong variation of the hole barrier height with temperature.

To improve the fit between the simulated and experimental I–V data at low biases, we introduced a discrete trap level into the MEH-PPV [21]. The trap level was placed at 0.3 eV above the HOMO level, with a trap concentration of 3.5×10^{22} m^{-3}. Figure 4 shows the effect of the trap level on the I–V characteristic at 300 K, where ϕ_{bp} was set to 0.37 eV,

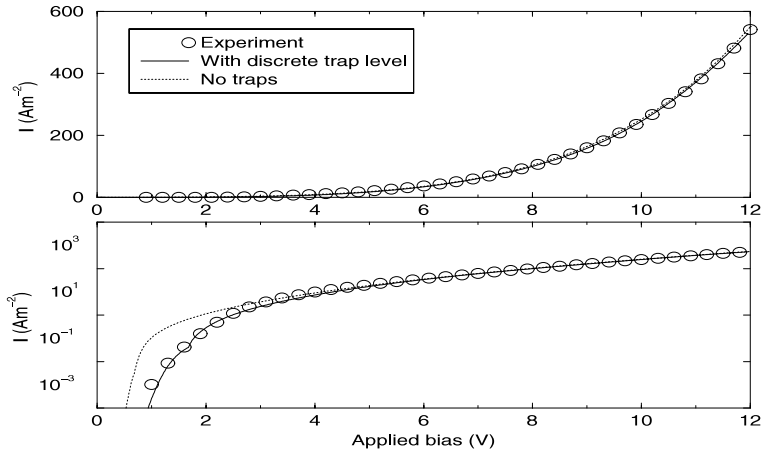

Figure 4. Comparison of simulated data, with and without a discrete trap level, to experimental data at 300 K.

$\mu_p = 3 \times 10^{-10}$ m^2 V^{-1} s^{-1} and $E_0 = 5 \times 10^9$ V m^{-1}. As can be seen from figure 4, the trap level clearly improves the fit to the experimental data at low bias, by reducing the current compared to the situation without a trap level present. However, at lower temperatures, the model provides too low a current at low biases compared to the experimental data without traps (see figure 1), making the fit to experimental data worse. On the basis of these results, we conclude that either there are no deep trap levels present in the material—this would concur with the conclusions of Scott *et al* [10]—or that traps are introduced at higher temperatures, e.g. because of changes in the conformational disorder in the material [22].

Another device characteristic investigated was the internal efficiency, η, given by

$$\eta = I_R/I \tag{5}$$

where the recombination current, I_R, is

$$I_R = \int_{x=0}^{x=l} qR\,\mathrm{d}x = I_p(0) - I_p(l) = I_n(l) - I_n(0) \tag{6}$$

where $I_p(0)(I_n(0))$ is the hole (electron) current at the anode (i.e. at $x = 0$) and $I_p(l)(I_n(l))$ is the hole (electron) current at the cathode (i.e. at $x = l$), and assuming that the holes are injected at the left hand electrode, and electrons are injected at the right hand electrode. As η can only be predicted with a bipolar model, fitting it gives us an opportunity to look at the variation of ϕ_{bn} with temperature.

Assuming the device efficiency to be the light output divided by the current, the experimental data, plotted in the top panel of figure 5, shows that upon cooling from 300 to 11 K, the device efficiency increases by a factor of about 40. We only modelled the device efficiency over a temperature range of 200–300 K, as the results from figure 1 suggest that the drift-diffusion model is not likely to be valid below 200 K and these results are shown in the lower panel. The electron mobility, μ_n, was assumed to be either $0.1\mu_p$ or $0.01\mu_p$ owing to MEH-PPV being a preferential hole transporter, and the barrier to electron injection was initially set at 1.3 eV at 300 K. In order to increase the efficiency as the temperature was decreased, ϕ_{bn} had to be lowered at each temperature by the amount shown in figure 5. We have no information about the parameters that determine μ_n as noted at the beginning of this section. Fortunately, the only predictions which could be sensitive to μ_n are those in figure 5. We have therefore examined two values for μ_n to check this point. It is clear from the results

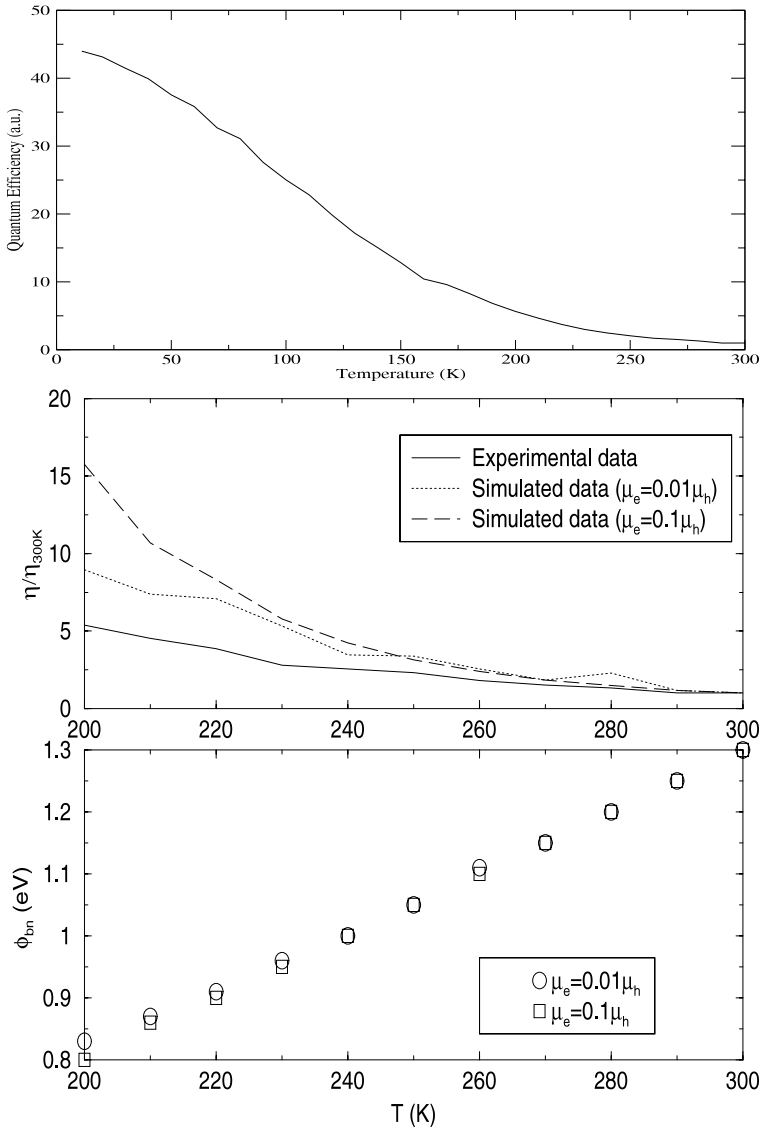

Figure 5. Top panel: experimental device efficiencies at a bias of 13 V (au) over a temperature range of 11–300 K. Simulated and fitted device efficiencies (middle panel) and electron barrier heights (ϕ_{bn}) (bottom panel) at a bias of 10 V and a temperature range of 200–300 K.

that it is the device efficiency, and not the barrier height, that is sensitive to μ_n, suggesting that the efficiency is affected by bulk transport as well as by injection over the barrier. In practice, μ_n is likely to decrease more rapidly as the temperature decreases than μ_p because it is more sensitive to the disorder in this material, but this would lead to transport which is less balanced between electrons and holes and so give a decrease in efficiency. We therefore cannot comment on how bulk transport influences the efficiency without quantitative information about how μ_n varies with temperature.

Although the model did show increased efficiency as the temperature was lowered, the slope of the curve in figure 5 is much steeper (5 meV K^{-1}) than that in figure 2 (1 meV K^{-1}).

A smaller slope gives rise to an efficiency which decreases as the temperature is lowered. This result is a further indication that, although the bandgap does indeed decrease with temperature as previously discussed, this cannot fully account for our observations since the sum of the changes in the barrier heights is greater than the observed bandgap shrinkage. The device efficiencies were recalculated assuming that ϕ_{bn} was 1 eV at 300 K. When the barrier height was fitted as a function of temperature, exactly the same slope was obtained.

4. Conclusions

From the fitting of the simulation parameters to the experimental data, we have found the values of $\Delta = 0.27$ eV, $\mu_0 = 1 \times 10^{-5}$ m^2 V^{-1} s^{-1}, $T_0 = 325$ K and $B = 1.3 \times 10^{-5}$ eV mV$^{-1/2}$ for this sample of MEH-PPV. Although the model provides good fits to the data at temperatures of 200–300 K, the poorer fits to the data at 150 K, and our difficulty in explaining the observed temperature gradients of the hole and electron barrier heights, means that more work needs to be carried out in understanding injection into organic devices. Baldo and Forrest [23] have proposed a model in which injection is limited by charge hopping out of interfacial molecular sites, whose energy distribution is broadened by local disorder in the interfacial dipole field and this could be a possible explanation. On the microscopic scale, injection into disordered molecular semiconductors has been studied by [24, 25]. These authors have shown that the results from a microscopic injection simulation qualitatively resemble both FN tunnelling-type currents and Richardson–Schottky thermionic emission currents. Thus it is arguable that the agreement between the microscopic and macroscopic injection terms is good enough, particularly at high temperatures, and that the macroscopic models can be used with confidence to aid device design. However, the problems in obtaining useful results from the macroscopic model at low temperatures and with modelling electron transport demonstrate the need for a more accurate model that can circumvent these difficulties.

Acknowledgments

SJM would like to thank the Engineering and Physical Sciences Research Council and Sharp Laboratories of Europe for a studentship. IDWS is a Royal Society University Research Fellow.

References

[1] Burroughes J H, Bradley D D C, Brown A R, Marks R N, Mackay K, Friend R H and Burns P L 1990 *Nature* **347** 539–41
[2] Tang C W and van Slyke S A 1987 *Appl. Phys. Lett.* **51** 913
[3] Blades C D J and Walker A B 2000 *Synth. Met.* **111–112** 335
[4] Martin S J, Verschoor G L B, Webster M A and Walker A B 2002 *Org. Electron.* at press
[5] Davids P S, Campbell I H and Smith D L 1997 *J. Appl. Phys.* **82** 6319
[6] Malliaras G G and Scott J C 1998 *J. Appl. Phys.* **83** 5399
[7] Blom P W M and de Jong M J M 1999 *IEEE J. Sel. Top. Quantum Electron.* **4** 105
[8] Lupton J M and Samuel I D W 1999 *J. Phys. D: Appl. Phys.* **32** 2973
[9] Lupton J M and Samuel I D W 2000 *Synth. Met.* **111–112** 381
[10] Scott J C, Brock P J, Salem J R, Ramos S, Malliaras G G, Carter S A and Bozano L 2000 *Synth. Met.* **111–112** 289
[11] Malliaras G G, Salem J R, Brock P J and Scott J C 1998 *Phys. Rev.* B **58** R13 411
[12] Bässler H 2000 *Semiconducting Polymers: Chemistry, Physics and Engineering* ed G Hadziioannou and P F van Hutten (Weinheim: Wiley–VCH)
[13] Mott N F and Davis E A 1971 *Electronic Processes in Noncrystalline Materials* (Oxford: Clarendon)
[14] Bozano L, Carter S A, Scott J C, Malliaras G G and Brock P J 1999 *Appl. Phys. Lett.* **74** 1132

[15] Campbell I H, Hagler T W, Smith D L and Ferraris J P 1996 *Phys. Rev. Lett.* **76** 1900
[16] Koehler M, de Lima J R, da Luz M G E and Hummelgen I A 1999 *Phys. Status Solidi* a **173** 29
[17] Blom P W M, de Jong M J M and van Munster M G 1997 *Phys. Rev.* B **55** 656
[18] Blades C D J 2000 *PhD Thesis* University of Bath
[19] Murgatroyd P N 1970 *J. Phys. D: Appl. Phys.* **3** 151
[20] Lupton J M 2002 *Appl. Phys. Lett.* **80** 186
[21] Stallinga P, Gomes H L, Rost H, Holmes A B, Harrison M G and Friend R H 2000 *Synth. Met.* **111–112** 535
[22] Sheridan A K, Lupton J M, Samuel I D W and Bradley D D C 2000 *Synth. Met.* **111–112** 531
[23] Baldo M A and Forrest S R 2001 *Phys. Rev.* B **64** 085201
[24] Arkhipov V I, Emelianova E V, Tak Y H and Bässler H 1998 *J. Appl. Phys.* **84** 848
[25] Wolf U, Arkhipov V I and Bässler H 1999 *Phys. Rev.* B **59** 7507